JSHC
Japan Society of Histochemistry and Cytochemistry
Established 1959

Acta Histochem. Cytochem. 42 (4): 121–128, 2009
doi:10.1267/ahc.09006

The Effects of Diuretics on Intracellular Ca^{2+} Dynamics of Arteriole Smooth Muscles as Revealed by Laser Confocal Microscopy

Yasunori Tamagawa[1], Tomoyuki Saino[1], Makoto Matsuura[2] and Yoh-ichi Satoh[1]

[1]Department of Anatomy (Cell Biology), School of Medicine, Iwate Medical University and [2]Department of Advanced Pharmaceutics, School of Pharmacy, Iwate Medical University, Morioka 020–8505, Japan

Received February 26, 2009; accepted June 12, 2009; published online August 11, 2009

The regulation of cytosolic Ca^{2+} homeostasis is essential for cells, including vascular smooth muscle cells. Arterial tone, which underlies the maintenance of peripheral resistance in the circulation, is a major contributor to the control of blood pressure. Diuretics may regulate intracellular Ca^{2+} concentration ($[Ca^{2+}]_i$) and have an effect on vascular tone. In order to investigate the influence of diuretics on peripheral resistance in circulation, we investigated the alteration of $[Ca^{2+}]_i$ in testicular arterioles with respect to several categories of diuretics using real-time confocal laser scanning microscopy. In this study, hydrochlorothiazide (100 μM) and furosemide (100 μM) had no effect on the $[Ca^{2+}]_i$ dynamics. However, when spironolactone (300 μM) was applied, the $[Ca^{2+}]_i$ of smooth muscles increased. The response was considerably inhibited under either extracellular Ca^{2+}-free conditions, the presence of Gd^{3+}, or with a treatment of diltiazem. After the thapsigargin-induced depletion of internal Ca^{2+} store, the spironolactone-induced $[Ca^{2+}]_i$ dynamics was slightly inhibited. Therefore, the spironolactone-induced dynamics of $[Ca^{2+}]_i$ can be caused by either a Ca^{2+} influx from extracellular fluid or Ca^{2+} mobilization from internal Ca^{2+} store, with the former being dominant. As tetraethylammonium, an inhibitor of the K^+ channel, slightly inhibited the spironolactone-induced $[Ca^{2+}]_i$ dynamics, the K^+ channel might play a minor role in those dynamics. Tetrodotoxin, a neurotoxic Na^+ channel blocker, had no effect, therefore the spironolactone-induced dynamics is a direct effect to smooth muscles, rather than an indirect effect via vessel nerves.

Key words: confocal microscopy, diuretics, intracellular calcium ion, testicular arterioles

I. Introduction

A diuretic-induced increase in the excretion of water from the body is used to treat heart failure, liver cirrhosis, hypertension and certain kidney diseases. Recent reports have suggested that the antihypertensive actions of some diuretics could not be due solely to a decrease in blood volume from increased urine production, but that dilatation of vessels must also play a role [3, 8, 9, 18, 24, 25]. However, the exact mechanism of the vasodilatation by diuretics is still an enigma. The resistance vessels (arterioles; less than ca. 100 μm in diameter) controls regional tissue circulation, and play a pivotal role in controlling systemic blood pressure. The effect of diuretics on arterioles has not been studied, while the diuretic-induced dilatation of veins was reported [3, 9, 18].

It is well established that the dynamics of intracellular Ca^{2+} concentration ($[Ca^{2+}]_i$) is fundamental in the regulation of various cellular functions [5], including the contraction of smooth muscles [2, 29, 33]. However, only a few studies on the $[Ca^{2+}]_i$ dynamics of arterioles are currently available, although these studies are very important for understanding the pathophysiology of hypertension as well as the pharmacology of drugs. Digital imaging analysis of the dynamics of $[Ca^{2+}]_i$ in intact living tissues composed of various cells may represent a useful approach for distinguishing the different

Correspondence to: Tomoyuki Saino, Department of Anatomy (Cell Biology), School of Medicine, Iwate Medical University, Uchimaru 19–1, Morioka 020–8505, Japan. E-mail: tsaino@iwate-med.ac.jp

responses to a transmitter. The best approach would be to study the dynamics between $[Ca^{2+}]_i$ and smooth muscles in intact arteriole specimens using real-time confocal microscopy [15–17, 26–28]. Thus far, we have succeeded in showing that either ATP, various proteases or 5-HT elicited a set of dynamics between $[Ca^{2+}]_i$ and arteriole smooth muscles, and that the responses were size- and organ-dependent [15, 17, 28].

The aim of the present study was to clarify the effects of some typical diuretics (hydrochlorothiazide, furosemide and spironolactone) on arterioles. To this end, we have analyzed the $[Ca^{2+}]_i$ dynamics of intact arterioles. We expected that diuretics would induce a decreased $[Ca^{2+}]_i$ following a decrease in vascular-tone and dilatation of the resistance vessels. Contrary to our expectations, in this study we found a diuretic-induced $[Ca^{2+}]_i$ increase in arteriole smooth muscles. The mechanism of the unexpected result will be discussed.

II. Materials and Methods

Preparation of arterioles

Experiments were conducted according to the guidelines of the ethics committee for animal treatment of Iwate Medical University. Adult male rats (Wistar, 8–12 weeks old, body weight 250–400 g) were euthanized by carbon dioxide gas. They were then perfused via the left cardiac ventricle with Ringer's solution (147 mM NaCl, 4 mM KCl and 2.25 mM $CaCl_2$) at room temperature (ca. 20–25°C) and a hydrostatic pressure of approximately 1 m of H_2O. After a wash-out of blood cells from the vessels, the testes were removed and placed in Hepes-buffered Ringer's solution (HR). The HR solution contained 118 mM NaCl; 4.7 mM KCl; 1.25 mM $CaCl_2$; 1.13 mM $MgCl_2$; 1 mM NaH_2PO_4; 5.5 mM D-glucose; MEM amino acid solution (Gibco, Grand Island, NY, USA); 0.2% bovine serum albumin (Sigma, St. Louis, MO, USA); and, 10 mM Hepes, adjusted with NaOH to pH 7.4. Arterial trees were isolated from testes, and connective tissues around vessels were carefully removed using fine forceps. The specimens were then incubated in HR containing purified collagenase (100 U/ml; Elastin Products, Owensville, MO, USA) for 2 hr at room temperature.

Scanning electron microscopy

We observed the arterioles by scanning electron microscopy (SEM). The isolated arterioles were fixed in 0.25% glutaraldehyde (Nacalai Tesque, Kyoto, Japan) and 4% paraformaldehyde (Merck KGaA, Darmstadt, Germany) in phosphate-buffered saline (0.1 M) for about 2 days at 4°C. The arterioles were then digested with KOH, followed by crude type II collagenase (Worthington, Lakewood, NJ, USA) [31]. The cells were post-fixed with 1% osmium tetroxide for 1 hr, and then dehydrated in a graded series of ethanol. Lastly, they were coated with platinum in an ion sputter coater (E-1030, Hitachi Co, Hitachi, Japan) and observed under a scanning electron microscope (S-2300; Hitachi Co).

Intracellular Ca^{2+} imaging

Live arteriole specimens were placed on a glass cover slip, set in a perfusion chamber and incubated with 10 μM Indo-1/AM (a Ca^{2+} sensitive fluorescent dye; Dojindo, Kumamoto, Japan) in the HR solution for 1 hr at 37°C. Indo-1 (excited by ultraviolet light) is a ratiometric dye that is used in the quantitative determination of $[Ca^{2+}]_i$. The emission maximum of Indo-1 shifted from 475 nm in Ca^{2+}-free medium to 400 nm when the dye solution was saturated with Ca^{2+}. A ratio of emission intensity that was shorter than 440 nm to one that was longer than 440 nm was used to estimate $[Ca^{2+}]_i$; the higher ratio indicated a higher $[Ca^{2+}]_i$. Artifacts that include photobleaching and/or dye leakage can be eliminated using this ratiometry. We measured the time course of $[Ca^{2+}]_i$ dynamics in restricted areas (region of interest; ROI). The area of the ROIs was approximately 3 μm^2.

A real-time confocal microscope (RCM/Ab; a modified version of a Nikon model RCM-8000, Tokyo, Japan) was used to measure the dynamics of $[Ca^{2+}]_i$. Cells loaded with Indo-1 were exposed to an ultraviolet-beam (351 nm). An argon-ion laser was equipped with an inverted microscope (TE-300, Nikon), and the fluorescence emission was passed through a water-immersion objective lens (Nikon C Apo 40×, N.A. 1.15) to a pinhole diaphragm. To decrease electrical noise and reduce photodamage, each image was integrated from eight frames, and sequential images were intermittently acquired every 1 sec, although the shortest acquisition time per image frame was 1/15 sec using this system. Images were immediately stored on high-speed hard disks. The digital images from the laser scanning microscopic imaging were composed of 512×480 pixels with a density resolution of 8 bits/pixel. The fluorescent intensity displayed 256 pseudo colors, with red representing the high $[Ca^{2+}]_i$ and purple and blue representing the low $[Ca^{2+}]_i$.

Perfusion

The $[Ca^{2+}]_i$ dynamics of arterioles was observed in a perfusion chamber as quickly as possible after the dye-loading. After perfusion with the standard HR for a few minutes, intact arterioles were selected and examined under the microscope. Arterioles which showed completely sufficient fluorescent signals were selected. Injured cells in the arterioles, which showed high $[Ca^{2+}]_i$ at resting conditions, were excluded from the subsequent temporal analyses.

After a brief washing with the HR, the specimens were continuously perfused with HR containing the following diuretics and modulators: hydrochlorothiazide (a blocker of the Na^+-Cl^- symporter of distal tubules of kidneys, 100 μM; Sigma); furosemide (a blocker of the Na^+-K^+-$2Cl^-$ symporter of the Henle loop of kidneys, 100 μM; Sigma); spironolactone (an antagonist to aldosterone, 300 μM; Wako, Japan); thapsigargin (a microsomal Ca^{2+}-ATPase inhibitor, 2 μM; Alomone Labs, Jerusalem, Israel); $GdCl_3$ (a nonspecific cation channel blocker, 100 μM; Wako, Japan); diltiazem (a L-type Ca^{2+} channel blocker, 50 μM; Sigma); tetraethylammonium (TEA: an inhibitor of the K^+ channel, 100 μM;

Sigma); and, tetrodotoxin (TTX: an inhibitor of the Na^+ channel, 100 nM; Sigma). Ca^{2+}-deficient solutions were removed from the solutions.

III. Results

Structure of arteriole specimens

Images of arterioles by SEM and real-time confocal laser scanning microscopy are shown in Figure 1. Arterioles were surrounded by spindle-shaped smooth muscles in a circular fashion. There was little morphological deterioration following the isolation procedures. Confocal laser scanning microscopy provided clear images showing smooth muscle profiles. Images obtained by ratiometry showed that the $[Ca^{2+}]_i$ in the arterioles was stable and that their ratio was about 0.5 in the absence of agonists.

Effect of diuretics on $[Ca^{2+}]_i$ dynamics

Arteriole specimens were perfused with normal HR for 5 min before administration of diuretics. During the unstimulated resting period, no spontaneous $[Ca^{2+}]_i$ dynamics of smooth muscles were observed.

When hydrochlorothiazide (100 μM) was added to the perfused HR, no dynamics of $[Ca^{2+}]_i$ were detected (Fig. 2). Furosemide (100 μM) induced no significant $[Ca^{2+}]_i$ dynamics (Fig. 3). To the contrary, spironolactone (300 μM) caused transient $[Ca^{2+}]_i$ dynamics. The response of $[Ca^{2+}]_i$ was biphasic; there was an initial rapid increase in $[Ca^{2+}]_i$, followed by a second gradual decline phase with fine oscillatory fluctuation (number of experiments; n=18) (Figs. 4, 5A). During the increase in $[Ca^{2+}]_i$, smooth muscles contraction was evident, and the external diameter decreased by approximately 20%.

Mechanism of spironolactone-induced $[Ca^{2+}]_i$ dynamics

There are two major mechanisms for increasing $[Ca^{2+}]_i$: (1) A Ca^{2+} influx via the ion channel of the plasma cell membrane, and, (2) a Ca^{2+} mobilization from internal Ca^{2+} stores (e.g., sarco-endoplasmic reticulum) [1]. To determine whether the Ca^{2+} influx correlated with the spironolactone-induced $[Ca^{2+}]_i$ increase, we observed the reaction under extracellular Ca^{2+}-free conditions (n=14) (Fig. 5B) in the presence of either a non-specific cation channel blocker (Gd^{3+}; 100 μM, n=12) (Fig. 5C) or an L-type Ca^{2+} channel blocker (diltiazem, 50 μM, n=14, data not shown). When the Ca^{2+} influx was inhibited under the conditions, the initial increase was considerably suppressed, and the slow decline phase disappeared (Fig. 5B, C). These data indicated that Ca^{2+} influx played a pivotal role in either the initial increase or the decline phase in spironolactone-induced $[Ca^{2+}]_i$ dynamics.

To investigate a possible contribution of Ca^{2+} mobilization from internal stores, thapsigargin was used (n=10). The depletion of Ca^{2+} stores by thapsigargin (2 μM) considerably inhibited the initial $[Ca^{2+}]_i$ increase, indicating that the mobilization correlates with the initial phase of spironolactone-induced $[Ca^{2+}]_i$ dynamics. Thapsigargin has few effects on the decline phase of spironolactone-induced $[Ca^{2+}]_i$ dynamics, consequently it is likely that the replenishment of Ca^{2+} from the external environment, but not Ca^{2+} mobilization, is essential in the decline phase.

Spironolactone is an agonist of aldosterone, which affects the transport of Na^+, K^+ and Cl^- in kidney epithelial cells. Therefore, we examined whether K^+ or Na^+ channels are correlated to the spironolactone-induced dynamics between $[Ca^{2+}]_i$ and smooth muscles. Tetraethylammonium (100 μM) partially inhibited the spironolactone-induced initial increase in $[Ca^{2+}]_i$, but the following oscillatory fluctua-

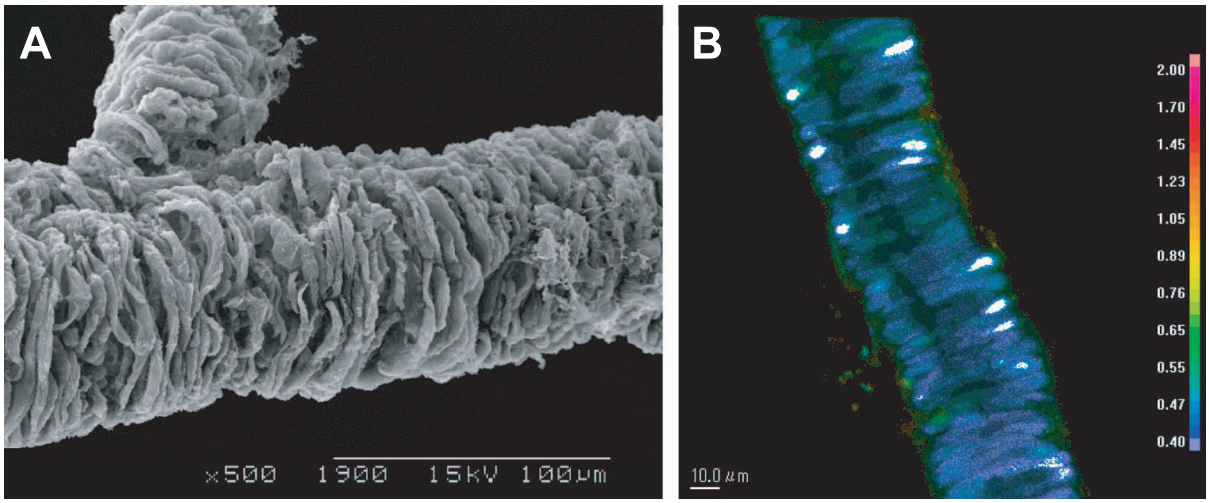

Fig. 1. Arteriole specimens from testicular tissue used in the present study. (**A**) Scanning electron micrograph. Bar=100 μm. (**B**) Confocal fluorescent image showing indo-1 ratio pseudocolor. Smooth muscles were shown as spindle-shaped profiles and maintained a circular arrangement. Damaged cells with a high $[Ca^{2+}]_i$ level were rare, ensuring functional integrity of the specimen. Bar=100 μm, Color scale bar=fluorescence ratio represents $[Ca^{2+}]_i$.

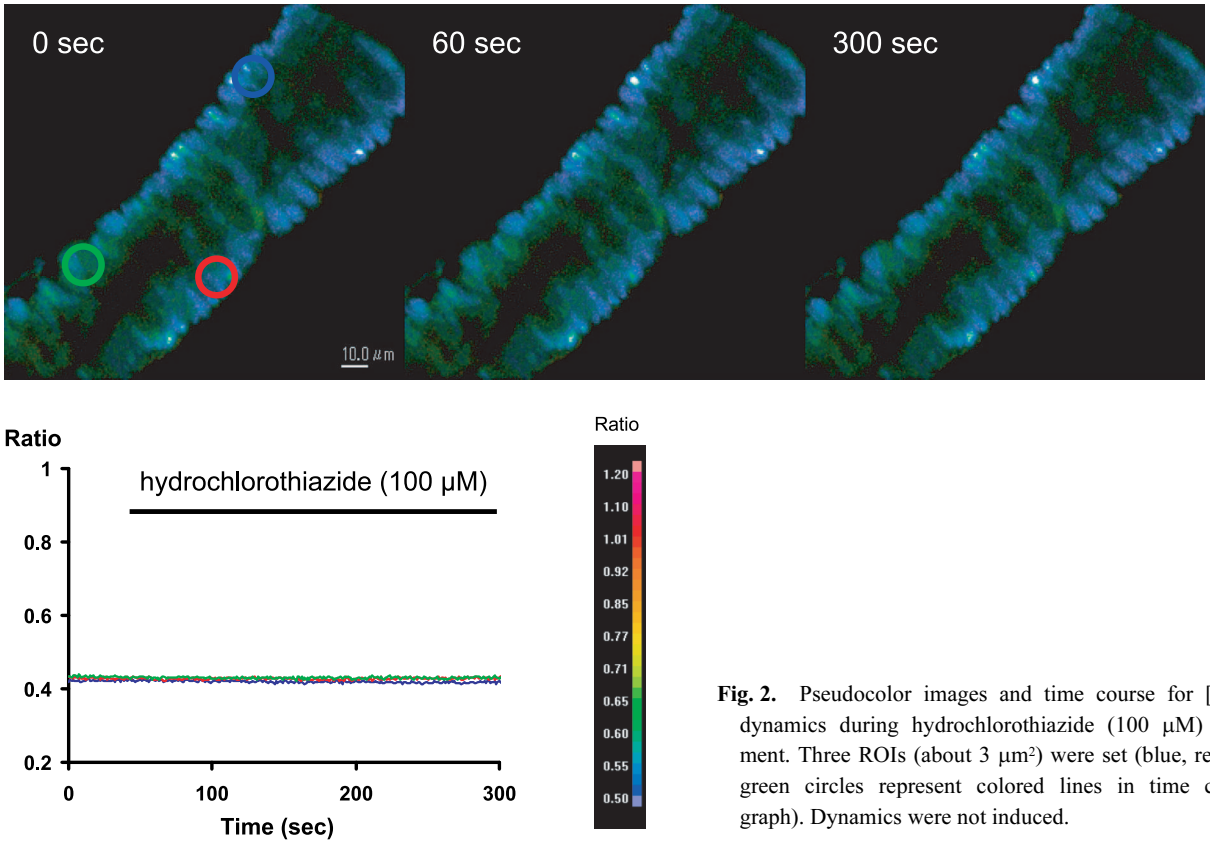

Fig. 2. Pseudocolor images and time course for $[Ca^{2+}]_i$ dynamics during hydrochlorothiazide (100 μM) treatment. Three ROIs (about 3 μm^2) were set (blue, red and green circles represent colored lines in time course graph). Dynamics were not induced.

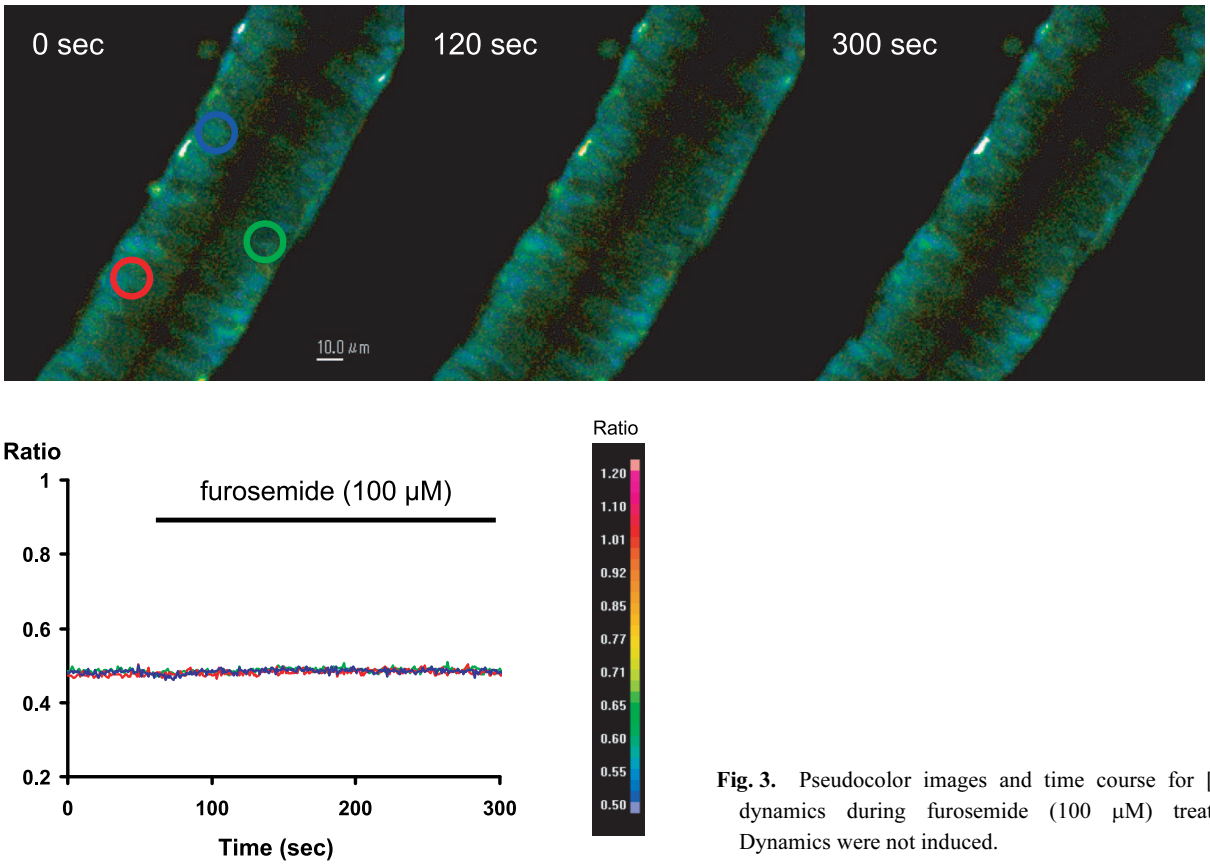

Fig. 3. Pseudocolor images and time course for $[Ca^{2+}]_i$ dynamics during furosemide (100 μM) treatment. Dynamics were not induced.

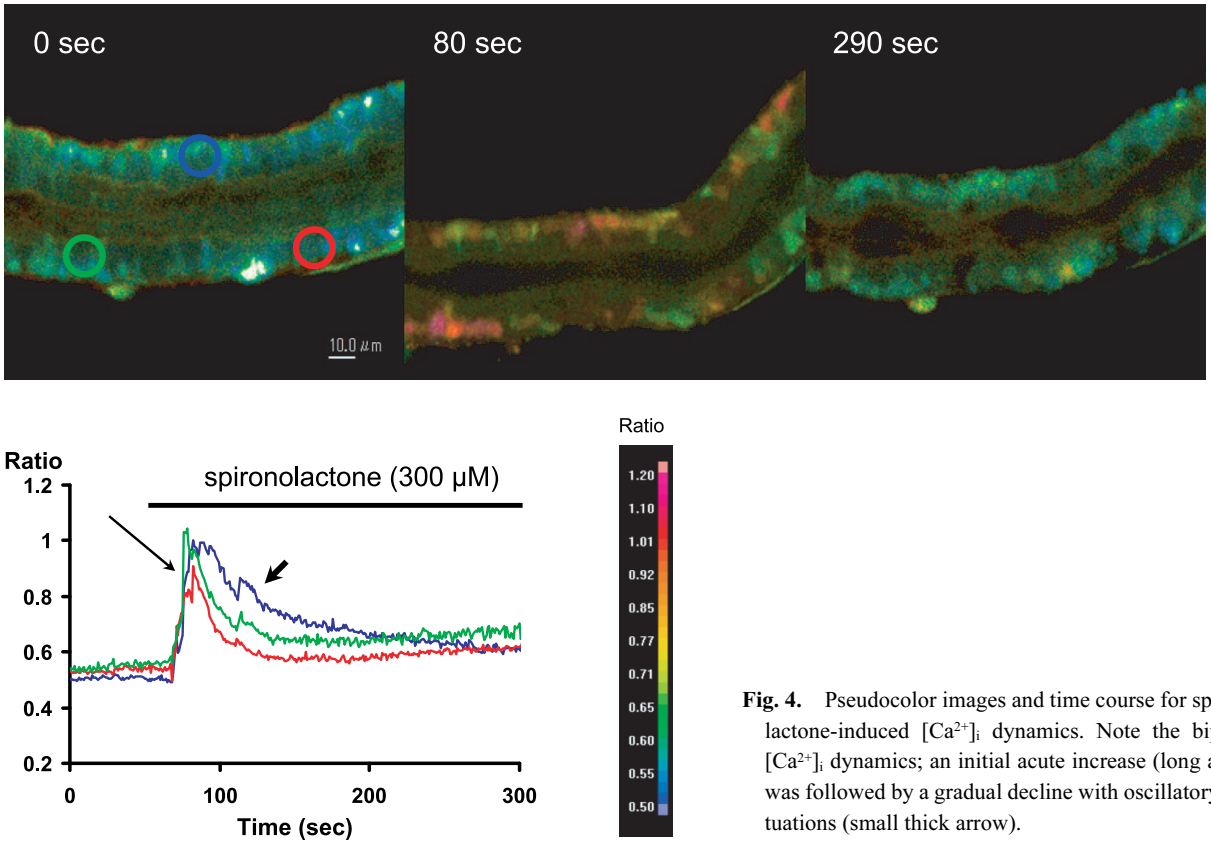

Fig. 4. Pseudocolor images and time course for spironolactone-induced $[Ca^{2+}]_i$ dynamics. Note the biphasic $[Ca^{2+}]_i$ dynamics; an initial acute increase (long arrow) was followed by a gradual decline with oscillatory fluctuations (small thick arrow).

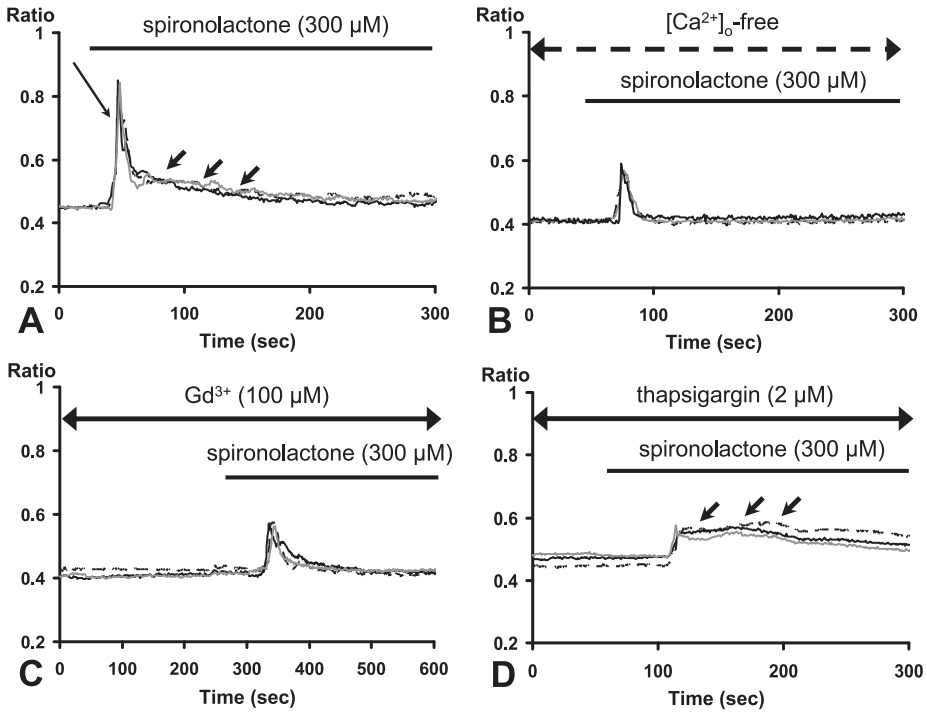

Fig. 5. Time courses for the spironolactone-induced $[Ca^{2+}]_i$ dynamics under various modulations. Temporal changes of $[Ca^{2+}]_i$ for three ROIs are depicted (black, gray and dotted lines). (**A**) positive controls (only spironolactone stimulation). The initial acute increase (long arrow) and a gradual decline (small thick arrow) are shown. (**B**) spironolactone-induced $[Ca^{2+}]_i$ dynamics under extracellular Ca^{2+}-free conditions ($[Ca^{2+}]_o$-free). (**C**) spironolactone-induced $[Ca^{2+}]_i$ dynamics in the presence of Gd^{3+} (100 μM). (**D**) spironolactone-induced $[Ca^{2+}]_i$ dynamics after depleting intracellular Ca^{2+} stores by treatment with thapsigargin (2 μM). A gradual decline (small thick arrow) are shown.

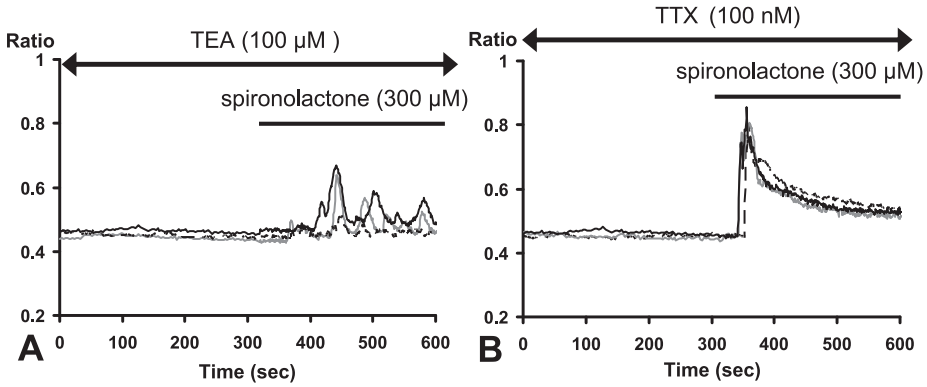

Fig. 6. Time courses for the spironolactone-induced $[Ca^{2+}]_i$ dynamics under channel blockers. (**A**) Effect of tetraethylammonium (TEA: 100 μM). (**B**) Effect of tetrodotoxin (TTX: 100 nM).

tions were observed (n=14) (Fig. 6A), indicating that the initial increase of spironolactone-induced $[Ca^{2+}]_i$ dynamics were affected by K^+ transport. Tetrodotoxin (TTX) binding physically blocks the flow of sodium ions through the channel, thereby preventing generation and propagation of action potential in excitable cells. TTX (100 μM) failed to inhibit the spironolactone-induced $[Ca^{2+}]_i$ dynamics (n=13) (Fig. 6B), which suggests that the generation of action potential was not necessary for a spironolactone-induced response. Our arteriole specimens contained autonomic nerve endings, therefore spironolactone might stimulate nerve endings and the released neurotransmitters would elicit the $[Ca^{2+}]_i$ dynamics, but the possibility can be excluded, because of the lack of an effect of TTX.

IV. Discussion

We verified the possible antihypertensive effects of diuretics on blood vessels. The results were contrary to our expectations; that is, a decreased $[Ca^{2+}]_i$ was not detected, and instead, spironolactone elicited an evident $[Ca^{2+}]_i$ increase with a resultant contraction of smooth muscles. Nevertheless, the present study is the first to reveal the involvement of the dynamics of $[Ca^{2+}]_i$ with respect to diuretics in intact peripheral arterioles.

Validity of the experimental procedure

When unexpected results are obtained, the verification of the validity of the experimental procedure is required. We used intact arteriole specimens rather than cultured smooth muscle cells derived from large elastic-type arteries (e.g., aorta). Ca^{2+} responses have been examined mainly in cultured and/or isolated vascular smooth muscles using various imaging techniques [4, 11, 12, 14, 36]. However, in the process of culturing the vascular smooth muscle cells, the biochemical properties of the contraction mechanism and the functional coupling between the sarco/endoplasmic reticulum and mitochondria were found to be altered during the dedifferentiation and/or the redifferentiation process that occurs with smooth muscle cells in culture [30, 32]. These isolated/cultured cells lose their natural conformation and structure, and the intracellular signaling of such cells can be altered [19].

The dynamics of $[Ca^{2+}]_i$ were analyzed using confocal microscopy in the present study. Photodamage and photobleaching under the general confocal microscope are severe, and can interfere with various cellular functions. We used a Nikon RCM which was equipped with a high-speed resonant galvanometer, allowing real-time image acquisition. We developed a monitoring system for photodamage [13], and faster scanning was empirically more effective for preventing photodamage. The objective was so bright that the excitation laser power could be set to the minimum. Various fine responses were detected using this system [28]. As a consequence, we are confident that the unexpected data were not caused by faulty experimental procedure.

Spironolactone-induced $[Ca^{2+}]_i$ increase

Spironolactone, a mineralocorticoid-receptor antagonist, prevents the detrimental effect of aldosterone, and although no resultant vasodilatations have ever been reported, it is known to induce hypotension on rare occasions [23]. Aldosterone-induced muscle contraction in clonal human smooth muscle cells was inhibited by spironolactone in *in vitro* experiments [10]. Surprisingly, in the present study spironolactone led to an increase in $[Ca^{2+}]_i$ in the smooth muscles of arterioles. Based on the present data, we concluded that the initial increase of the spironolactone-induced dynamics of $[Ca^{2+}]_i$ was caused by Ca^{2+} influx and Ca^{2+} mobilization, and that the subsequent decline phase with fine oscillatory fluctuations was correlated with the Ca^{2+} influx.

Various steroids can elicit vascular contraction [10], and activation of a plasma membrane receptor of aldosterone will induce the IP_3-mediated dynamics of $[Ca^{2+}]_i$ [35]. It is likely that spironolactone, having the same steroid nucleus, may transiently activate the membrane receptors. When all this is taken into account, and spironolactone is used as an antihypertensive drug, the possibility of the transient contraction of vessels in certain tissues must be considered.

No effect of thiazide and furosemide

Thiazide-like diuretics and furosemide have been the cornerstones of hypertension management for several years. Thiazide-like diuretics lower blood pressure by decreasing peripheral resistance rather than by their diuretic effect [34]. It has been suggested that thiazide-induced dilation of veins is mediated either by the opening of calcium-activated potassium channels or by the inhibition of carbonic anhydrase [6, 21, 22, 24, 25]. Intravenous administration of furosemide also induces a rapid dilation of veins with a decrease in ventricular pre-load that is responsible for the rapid improvement observed in patients with congestive heart failure, before the diuretic produces its effect [3, 9, 18]. Furosemide showed endothelium-dependent dilation of veins [7], while direct administration into the arteries had no dilative effect [8, 20]. These *in situ* experiments, however, lacked cell biological evidence. Our $[Ca^{2+}]_i$ analysis concerning the effect of hydrochlorothiazide and furosemide obtained in arteriole specimens can substantiate the previous reports [8, 20]. Further experiments will be necessary to completely clarify the relationship between dilative effects and intracellular signaling (e.g., cGMP or nitric oxide) in the smooth muscles of the arterial and venous systems.

Finally, further analysis of the $[Ca^{2+}]_i$ dynamics of arteriole smooth muscles during various steroidal stimulations and those of venous smooth muscles during the administration of different diuretics is required. The present imaging method using confocal microscopy will be a helpful tool to assay the effects of diuretics on intact vascular specimens.

Endothelial cells responses to diuretics

One may argue that endothelial cells play a role in $[Ca^{2+}]_i$ changes in arteriole smooth muscles. We observed $[Ca^{2+}]_i$ response of endothelial cells in testicular arterioles, but no response to diuretics was detected. Therefore, the participation of endothelial cells to the reactions can be neglected in the present study. However it will be necessary to do further experiments to clarify the relationship between smooth muscle cells and endothelial cells in arterioles.

V. Acknowledgements

We wish to express our thanks to K. Kumagai, Department of Histology, Iwate Medical University, for his skillful technical assistance. This work was supported in part by research grants from the Ministry of Education, Culture and Science of Japan (14770004), from the 2004 Intelligent Cosmos Foundation, and from the Promotion and Mutual Aid Corporation for Private Schools of Japan. A portion of this work was performed at the Advanced Medical Science Center of Iwate Medical University, which also provided financial support.

VI. References

1. Berridge, M. J., Bootman, M. D. and Roderick, H. L. (2003) Calcium signalling: dynamics, homeostasis and remodelling. *Nat. Rev. Mol. Cell Biol.* 4; 517–529.
2. Berridge, M. J. (2008) Smooth muscle cell calcium activation mechanisms. *J. Physiol.* 586; 5047–5061.
3. Biddle, T. L. and Yu, P. N. (1979) Effect of furosemide on hemodynamics and lung water in acute pulmonary edema secondary to myocardial infarction. *Am. J. Cardiol.* 43; 86–90.
4. Bolton, T. B. and Gordienko, D. V. (1998) Confocal imaging of calcium release events in single smooth muscle cells. *Acta Physiol. Scand.* 164; 567–575.
5. Bootman, M. D., Lipp, P. and Berridge, M. J. (2001) The organisation and functions of local Ca^{2+} signals. *J. Cell Sci.* 114; 2213–2222.
6. Calder, J. A., Schachter, M. and Sever, P. S. (1992) Direct vascular actions of hydrochlorothiazide and indapamide in isolated small vessels. *Eur. J. Pharmacol.* 220; 19–26.
7. Costa, M. A., Loria, A., Elesgaray, R., Balaszczuk, A. M. and Arranz, C. (2004) Role of nitric oxide pathway in hypotensive and renal effects of furosemide during extracellular volume expansion. *J. Hypertens.* 22; 1561–1569.
8. de Berrazueta, J. R., González, J. P., de Mier, I., Poveda, J. J. and García-Unzueta, M. T. (2007) Vasodilatory action of loop diuretics: a plethysmography study of endothelial function in forearm arteries and dorsal hand veins in hypertensive patients and controls. *J. Cardiovasc. Pharmacol.* 49; 90–95.
9. Dormans, T. P., Pickkers, P., Russel, F. G. and Smits, P. (1996) Vascular effects of loop diuretics. *Cardiovasc. Res.* 32; 988–997.
10. Gros, R., Ding, Q., Armstrong, S., O'Neil, C., Pickering, J. G. and Feldman, R. D. (2007) Rapid effects of aldosterone on clonal human vascular smooth muscle cells. *Am. J. Physiol. Cell. Physiol.* 292; C788–C794.
11. Iino, M., Kasai, H. and Yamazawa, T. (1994) Visualization of neural control of intracellular Ca^{2+} concentration in single vascular smooth muscle cells in situ. *EMBO J.* 13; 5026–5031.
12. Jaggar, J. H., Stevenson, A. S. and Nelson, M. T. (1998) Voltage dependence of Ca^{2+} sparks in intact cerebral arteries. *Am. J. Physiol.* 274; C1755–C1761.
13. Kuroda, T., Satoh, Y., Akutsu-Yamauchi, H., Shikanai, Y., Miyata, S., Saino, T., Russa, D., Habara, Y. and Cui, Z.-J. (2006) Quantitative analysis of photodamage during fluorescent bioimaging: monitoring of nitric oxide production using DAF-2. *Bioimages* 14; 9–18.
14. Li, Z., Zhang, Q., Zhao, S., Wei, M., Shenghui, Z., Cong, H., Ouda, H., Odajima, K. and Takemura, H. (1997) Responsiveness of cytosolic free calcium concentration in cultured rat pulmonary arterial smooth muscle cells: confocal microscopic measurement. *Res. Commun. Mol. Pathol. Pharmacol.* 97; 47–52.
15. Masu, K., Saino, T., Kuroda, T., Matsuura, M., Russa, A. D., Ishikita, N. and Satoh, Y. (2008) Regional differences in 5-HT receptors in cerebral and testicular arterioles of the rat as revealed by Ca^{2+} imaging of real-time confocal microscopy: variances by artery size and organ specificity. *Arch. Histol. Cytol.* 71; 291–302.
16. Matsuura, M., Saino, T. and Satoh, Y. (2004) Response to ATP is accompanied by a Ca^{2+} influx via P2X purinoceptors in the coronary arterioles of golden hamsters. *Arch. Histol. Cytol.* 67; 95–105.
17. Misaki, T., Satoh, Y., Saino, T. and Ogawa, A. (2006) The role of protease-activated receptors on the intracellular calcium ion dynamics of vascular smooth muscles, with special reference to cerebral arterioles. *Arch. Histol. Cytol.* 69; 49–60.
18. Mukherjee, S. K., Katz, M. A., Michael, U. F. and Ogden, D. A. (1981) Mechanisms of hemodynamic actions of furosemide: differentiation of vascular and renal effects on blood pressure in functionally anephric hypertensive patients. *Am. Heart J.* 101; 313–318.
19. Nelson, M. T., Patlak, J. B., Worley, J. F. and Standen, N. B. (1990) Calcium channels, potassium channels, and voltage dependence of arterial smooth muscle tone. *Am. J. Physiol.* 259;

C3–C18.
20. Pickkers, P., Dormans, T. P., Russel, F. G., Hughes, A. D., Thien, T., Schaper, N. and Smits, P. (1997) Direct vascular effects of furosemide in humans. *Circulation* 96; 1847–1852.
21. Pickkers, P., Hughes, A. D., Russel, F. G., Thien, T. and Smits, P. (1998) Thiazide-induced vasodilation in humans is mediated by potassium channel activation. *Hypertension* 32; 1071–1076.
22. Pickkers, P., Garcha, R. S., Schachter, M., Smits, P. and Hughes, A. D. (1999) Inhibition of carbonic anhydrase accounts for the direct vascular effects of hydrochlorothiazide. *Hypertension* 33; 1043–1048.
23. Pitt, B., Zannad, F., Remme, W. J., Cody, R., Castaigne, A., Perez, A., Palensky, J. and Wittes, J. (1999) The effect of spironolactone on morbidity and mortality in patients with severe heart failure. Randomized aldactone evaluation study investigators. *N. Engl. J. Med.* 341; 709–717.
24. Puscas, I., Coltau, M., Baican, M., Domuta, G. and Hecht, A. (1999) Vasodilatory effect of diuretics is dependent on inhibition of vascular smooth muscle carbonic anhydrase by a direct mechanism of action. *Drugs Exp. Clin. Res.* 25; 271–279.
25. Puscas, I., Coltau, M., Baican, M., Pasca, R., Domuta, G. and Hecht, A. (2001) Vasoconstrictive drugs increase carbonic anhydrase I in vascular smooth muscle while vasodilating drugs reduce the activity of this isozyme by a direct mechanism of action. *Drugs Exp. Clin. Res.* 27; 53–60.
26. Saino, T., Matsuura, M. and Satoh, Y. (2002) Application of real-time confocal microscopy to intracellular calcium ion dynamics in rat arterioles. *Histochem. Cell Biol.* 117; 295–305.
27. Saino, T., Matsuura, M. and Satoh, Y. (2002) Comparison of the effect of ATP on intracellular calcium ion dynamics between rat testicular and cerebral arteriole smooth muscle cells. *Cell Calcium* 32; 155–165.
28. Saino, T. and Satoh, Y. (2004) Application of real-time confocal laser scanning microscopy to observe living cells in tissue specimens. *J. Electron Microsc. (Tokyo)* 53; 49–56.
29. Somlyo, A. P. and Somlyo, A. V. (1994) Signal transduction and regulation in smooth muscle. *Nature* 372; 231–236.
30. Ueki, N., Sobue, K., Kanda, K., Hada, T. and Higashino, K. (1987) Expression of high and low molecular weight caldesmons during phenotypic modulation of smooth muscle cells. *Proc. Natl. Acad. Sci. U S A* 84; 9049–9053.
31. Ushiwata, I. and Ushiki, T. (1990) Cytoarchitecture of the smooth muscles and pericytes of rat cerebral blood vessels. A scanning electron microscopic study. *J. Neurosurg.* 73; 82–90.
32. Vallot, O., Combettes, L. and Lompre, A. M. (2001) Functional coupling between the caffeine/ryanodine-sensitive Ca^{2+} store and mitochondria in rat aortic smooth muscle cells. *Biochem. J.* 357; 363–371.
33. van Breemen, C. and Saida, K. (1989) Cellular mechanisms regulating $[Ca^{2+}]_i$ smooth muscle. *Annu. Rev. Physiol.* 51; 315–329.
34. van Brummelen, P., Man in 't Veld, A. J. and Schalekamp, M. A. (1980) Hemodynamic changes during long-term thiazide treatment of essential hypertension in responders and nonresponders. *Clin. Pharmacol. Ther.* 27; 328–336.
35. Wehling, M. (2005) Effects of aldosterone and mineralocorticoid receptor blockade on intracellular electrolytes. *Heart Fail. Rev.* 10; 39–46.
36. Yip, K. P. and Marsh, D. J. (1996) $[Ca^{2+}]_i$ in rat afferent arteriole during constriction measured with confocal fluorescence microscopy. *Am. J. Physiol.* 271; F1004–F1011.